Maejo International Journal of Energy and Environmental Communication

Journal homepage: https://ph02.tci-thaijo.org/index.php/MIJEEC

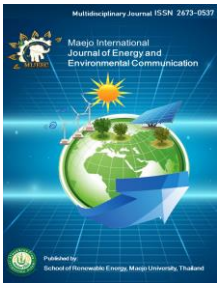

ARTICLE

Image analysis reveals cellular fragmentation of *Spirulina platensis* upon treatment with heavy metal ions

Lekha Kaushik[1*], Dinakari Sarangan[1*], Deenadayalan Karaiyagowder Govindarajan[1,2*], Sowmiya Muthumanickam[1], Muthusaravanan Sivaramakrishnan[1,3], Ram Kothandan[3], Suganthy Masanamani[1], Saraswathy Nachimuthu[1], Hadas Mamane[4], and Kumaravel Kandaswamy[1,2†].

[1]Laboratory of Molecular Biology and Genetic Engineering, Department of Biotechnology, Kumaraguru College of Technology, Coimbatore, Tamil Nadu, India.
[2]Research Center for Excellence in Microscopy, Department of Biotechnology, Kumaraguru College of Technology, Coimbatore 641049, Tamil Nadu, India.
[3]Laboratory of Bioinformatics, Department of Biotechnology, Kumaraguru College of Technology, Coimbatore, Tamil Nadu, India.
[4]Environmental Engineering Program, School of Mechanical Engineering, Faculty of Engineering, Tel Aviv University, Israel.

ARTICLEINFO

Article history:
Received 28 January 2022
Received in revised form
26 March 2022
Accepted 21 April 2022

Keywords:
Bioimaging
Cell Biology
Environmental monitoring
Image analysis
Microscopy

ABSTRACT

Bioremediation is a promising technique that can be used to decrease the environmental discharge of Heavy Metal (HM) such as copper, and zinc. Although studies have addressed the cytotoxic effects of HMs, the effect of HMs on the geometry of bacterial species such as *Spirulina platensis* (*S. platensis*) remains unknown. Quantitative analysis of parameters such as cell perimeter, cell count, and cell distribution shall greatly improve the efficiency of environmental monitoring. Therefore, this study demonstrates the use of an open-source image analysis tool (ImageJ/Fiji) to quantify the aforementioned parameters to analyze the extent of damage caused by lethal concentration of > 2 mg/L of Cu^{2+} and > 6 mg/L of Zn^{2+} which disintegrates *S. platensis* cells into smaller fragments and subsequently affects their structural parameters in perimeter and cell distribution. In summary, this article demonstrates the use of an image analysis platform to quantify the geometric parameters of microbes for environmental monitoring.

1. Introduction

Heavy Metals (HM) such as copper and zinc are major environmental pollutants in water bodies whose toxicity affects the physiological and biochemical characteristics of microbes (Tchounwou et al., 2012). *Spirulina platensis* (*S. Platensis*) is a cyanobacterium and proved to reduce environmental zinc sorption and effective biodegradation of alkyl benzene sulfonate, studies suggest that alkylbenzene sulfonate enhances *S. Platensis* to consume Zn^{2+} maximum of 4 mg/L and beyond the maximum concentration, the cell damage remains unknown (Meng et al., 2012; Palanisamy et al., 2021). Another study showed that optimum HM consumed by S. *Platensis* without any treatment, reveals that 2.5 mg/L of copper and 0.5 mg / L of zinc can be consumed by *S. Platensis* cells for optimal cell growth. However, higher concentrations (copper > 2.5 mg/L and zinc > 0.5 mg/L)

* Corresponding author.
E-mail address: kumaravel.k.bt@kct.ac.in (Kumarvel Kandaswamy)

become toxic to bacterial cells (Cepoi et al., 2020). In recent years, HM contamination in the environment was reduced using microbial remediation strategies such as bioaccumulation, biotransformation, biosorption, and biomineralization (Ayangbenro et al., 2017). Bioaccumulation is one such important process in which *S. platensis* can consume extracellular metals to a maximum of 283 mg/g chromium and 1.04 mg/g of zinc at pH 8.9 (Zinicovscaia et al., 2019). Taken together, the physical well-being of *S. Platensis* is crucial for it to consume the extracellular HMs. Studies were conducted to examine the toxic effect of external agents (such as ozone) on *S. Platensis* morphology (Coltelli et al., 2014), however, the toxic effect of HMs on *S. Platensis* cell morphology remains unknown. Therefore, imaging techniques such as phase-contrast microscopy and high-throughput image analysis were effective in quantifying the changes in *S. platensis* cell morphology during HM consumption.

Environmental monitoring is essential to maintain the ecological homeostasis between the microbes and HM during the bioaccumulation process (Coltelli et al., 2014). Algae are the known indicators for the water ecosystem, as they show a strong response to the changes in parameters such as nutrient enrichment, pH changes, suspended sediments, and organic contaminants. The lifespan of algae was about 6 to 8 weeks and they need to meet the nutritional requirements less than a day for it to enter their developmental phase (Coltelli et al., 2014; Bhuyar et al., 2019). To date, the metrics used for water quality monitoring were predominantly salinity, pH, and turbidity (Coltelli et al., 2014; Bhuyar et al., 2021). In moving forward, geometric parameters such as trichome perimeter, cell number, and cell distribution of microbes should be quantified to better assess the morphology and physical well-being of algal species. *S. platensis* possesses left-hand helix trichrome (spirals) which multiplies by binary fission (Ali et al., 2012). During development, *S. platensis* undergoes various morphological changes and produces either long or short spirals with varying helix pitch that affects its overall structural rigidity (Ali et al., 2012). Therefore, it is crucial to quantify the geometrical parameters to get a better understanding of cellular well-being.

Microscopy coupled with image analysis has allowed us to both visualize and quantify phenotypic characteristics of cells such as cell growth, count, shape, and size (Georg et al., 2018). Furthermore, image analysis tools such as ImageJ allows researchers to quantify the datasets in a high throughput manner (Schindelin et al., 2012). Alongside, a MATLAB-based image analysis platform named Projected System of Internal Coordinates from Interpolated Contours (PSICIC) was developed (Guberman et al., 2008) and implemented to quantify protein localization in bacterial cells of *Enterococcus faecalis* (Kandaswamy et al., 2013; Govindarajan et al., 2022) and biophysical changes in the bacterial cell membrane (Chilambi et al., 2020). ImageJ however has an advantage as it can read many file formats (eg. Tiff, Jpeg, Png) and perform statistical analysis of user-defined parameters. For instance, ImageJ has been implemented to analyse the particle size and shape of the talc powder (Rishi et al., 2015). In the biological system, it is necessary to track the phenotype of bacterial cells to exert their cell function (Ghensi et al., 2017). Therefore, quantitative image analysis tools provide numerous advantages over other cell sorting in various fields such as diseases prediction (Karthiyayini et al., 2020), biofuel applications (Akao et al., 2019), environmental quality monitoring (Coltelli et al., 2014), food quality monitoring (Bezuidenhout, 2018), and fluorescent labelled cells in microfluidic devices (Sivaramakrishnan et al., 2020). In this study, we have employed ImageJ/Fiji to quantify the trichome perimeter, cell number, and cell distribution of *S. Platensis*. Our results indicate that *S. Platensis* when treated HMs treatment promotes their growth and structural rigidity at lower concentrations ($Cu^{2+} \leq 2$ mg/L and $Zn^{2+} \leq 6$ mg/L) but becomes toxic and leads to fragmented cellular structure at high concentrations ($Cu^{2+} > 2$ mg/L and $Zn^{2+} > 6$ mg/L). Therefore, this study demonstrates the use of microscopy and image analysis as a potent tool for the rapid monitoring of environmental pollutants.

2. Material and Methods

2.1 Growth condition of Spirulina platensis

Spirulina platensis (*S. platensis*) culture was obtained from Sparkling Spirulina Farms (Pillayarpatti, Tamil Nadu, India). The strains were grown in Zarrouk's media, consists of 29.4 mM $NaNO_3$, 2.87 mM K_2HPO_4, 5.74 mM K_2SO_4, 17.1 mM NaCl, 0.81 mM $MgSO_4.7H_2O$, 0.27 mM $CaCl_2.2H_2O$, 0.036 mM $FeSO_4.2H_2O$, 0.27 mM EDTA and 199.8 mM $NaHCO_3$ at room temperature. The pH was maintained between 9 to 11. The flasks were agitated 3 to 4 times clockwise and anticlockwise daily. The culture was exposed to alternate light and dark periods every day (Wang et al., 2005). The culture was centrifuged (Remi C – 24 BL Cooling centrifuge) at 5000 rpm for 10 min at room temperature to pellet the cells. Finally, the pellets were resuspended by adding fresh media for subculture production.

2.2 Sample preparation for microscopy

For microscopy studies, the cell pellets were washed twice with 1 ml of 1X PBS buffer and resuspended with 1 ml of PBS during the final wash. Twenty microliters of this sample were taken and smeared on poly-L-lysine coated slides and air-dried for 15 min at room temperature. After the smear was air-dried, a drop of mounting media was added. A cover glass was placed over slides and sealed with nail polish on all four corners. The slides were then stored in the dark at 4 °C. The imaging was carried out in 4X magnification and taken for image analysis using ImageJ. Three images from three independent experiments were taken into consideration for image analysis analyses.

2.3 Treatment of S. platensis with $CuSO_4$ and $ZnSO_4$

To investigate the HM effect on the geometrical parameters, the *S. Platensis* was allowed to grow in a controlled environment allowing the exposure of sunlight for 21 days using Zarrouk's media. To observe the effects of HM, Zarrouk's media was supplemented with different concentrations of $CuSO_4$ (0, 1, 2, 3, 4, and 5 mg/L) and $ZnSO_4$ (0, 2, 4, 6, 8, and 10 mg/L) prior inoculation of *S. Platensis* and allowed to grow for 21 days. The samples were then examined in an optical microscope (Olympus CKX53 microscope) to track the changes in cell morphology due to HM stress.

2.4 Image analysis using ImageJ

For analysis in ImageJ, the brightfield images were converted to 8 bit, and thresholding was performed manually using the

threshold option to reduce the noise in microscopic images and to identify cell boundaries. The parameter such as cell perimeter, cell count, cell distribution was chosen for analysis. The cells were analyzed using the outline option to quantify entire cells in a single image. Post thresholding, an image was generated where the cell trichome outlines were labeled with cell number which was manually compared with obtained measurements results. The data can be exported to excel and sorted manually. ImageJ analysis was performed to obtain data directly in µm for perimeter as the scale. The artifacts were manually excluded in using a spreadsheet file extracted post-analysis from ImageJ (Collins, 2007).

3.0 Results And Discussion

3.1 S.platensis of varying cell length can be found during their growth phase

The *S. Platensis* cells were imaged in a phase-contrast microscope at 4X magnification. Then, the images were analyzed in ImageJ to quantify perimeter and cell distribution. The trichomes (Spirulina with spirals) were manually sorted based on the trichomes into three categories S1, S2, and S3. Where S1 are cells with perimeter <1 μ m, S2 are cell with perimeter $1 \leq P \leq 1.5$ μ m, and S3 are cells with perimeter >1.5 μ m, respectively (Figure 1), where P indicates perimeter of cells. The number of cells in each category was measured and compared with Zn^{2+} and Cu^{2+} treated cells and untreated cells (Figure 2). Therefore, in control samples, the number of cells having spirals between $1 \leq P \leq 1.5$ µm, perimeter (S_2 category) in their trichome stage was found to be significantly higher as a maximum of 5 cells than S_1 category (4 cells), and S_3 (4 cells) (Figure 3&4).

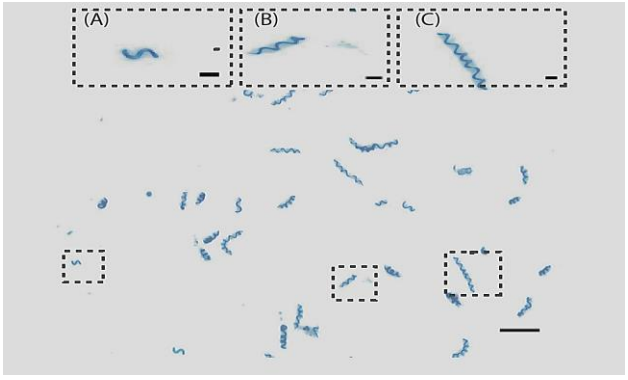

Figure 1 Bright-field images of *spirulina platensis*, scale bar 100 µm. Insets (A),(B), and (C) represented the siprulina population was subcategorized as S_1 (P<1 µm), S_2 (1 µm ≤ P ≤1.5 µm), and S_3 (P > 1.5 µm), respectively, where P denotes the perimeter of Spirals, and the inset scale bar is 10 µm.

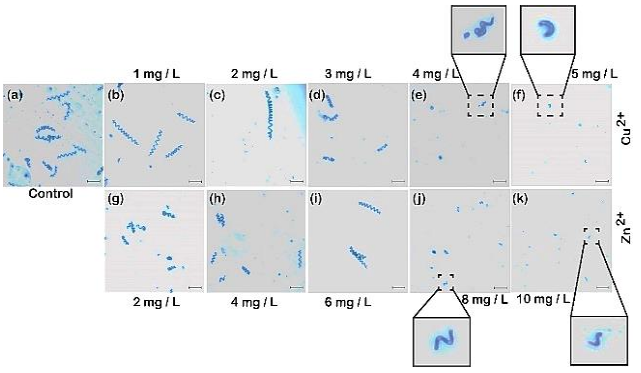

Figure 2 Zn^{2+} and Cu^{2+} cleaves the spiral sturctures of *S. Platensis*: (a) The *S. Platensis* cells grown in control samples; (b)(c) lower Cu^{2+} concentrations such as 1 mg /L, 2 mg /L promotes the *S. Platensis* cell growth, (d)(e)(f) higher Cu^{2+} concentrations such as 3 mg /L, 4 mg /L, 5 mg / L causes *S. Platensis* cell damage i.e., breaking spiral structure into fragments; similarly, (g)(h)(i) lower Zn^{2+} concentrations such as 2 mg /L, 4 mg /L and 6 mg / L promotes the *S. Platensis* cell growth; (j)(k) higher Zn^{2+} concentrations such as 8 mg /L and 10 mg /L causes *S. Platensis* cell damage i.e., breaking spiral structure into fragments.

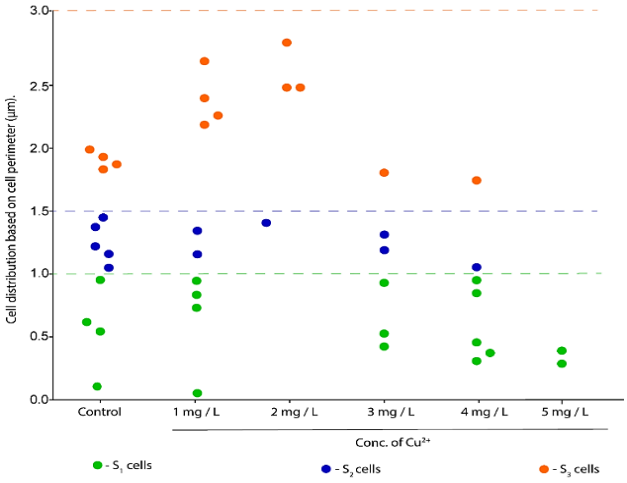

Figure 3 Cu^{2+} alters the *S. Platensis* cell population: In HM treatment, >2mg/L of Cu^{2+} breaks the S_3 cell population into smaller fragments and distributer smaller perimeter categories like S_2 and S_1. When the Zn^{2+} increases with fragmenting the cells into smaller fragments.

3.2 Cu^{2+} and Zn^{2+} cause both elongation and disintegrates of S.platensis

To quantify the effect of metal ions Cu^{2+} (from $CuSO_4$) and Zn^{2+} (from $ZnSO_4$) on *S. platensis* cell shape, the cells were treated with lethal concentration 1-5mg/L and 2-10mg/L of Cu^{2+} and Zn^{2+}, respectively (Figure 2). To perform image analysis, the cells treated with Cu^{2+} were grouped into three (S_1, S_2, and S_3) categories according to their cell perimeter shown (Figure 1). In the control (untreated) sample, there equal distribution of cells of all perimeter

(S_1= 4 cells, S_2= 5 cells, and S_3= 4 cells). At lower concentration 2 mg/L of Cu^{2+}, only cells at category S_3 were found to be more (3 cells) when compared to the S_2 category (1 cell). However, at a higher concentration of 5 mg/L of Cu^{2+}, only cells at category S_1= 2 cells were found. Taken together, it is clear that a lower concentration of Cu^{2+} (≤ 2 mg/L) promotes cell growth as evident by an increase in cell perimeter, however, a higher concentration of Cu^{2+} (> 2 mg/L) disintegrates the S_3 cells and is distributed to the S_1 category. This is in good agreement with a study conducted where they found *Spirulina* sp. fragmentation when treated with Cu^{2+} and NaCl (Deniz et al., 2011). In another study, it was shown that $CuSO_4$ treated *S. Plantensis* resulted in a reduction in the number of spirals (Choudhary et al., 2007). Taken together, our result indicates that a higher concentration of HM results in morphological changes to *S. platensis* cells.

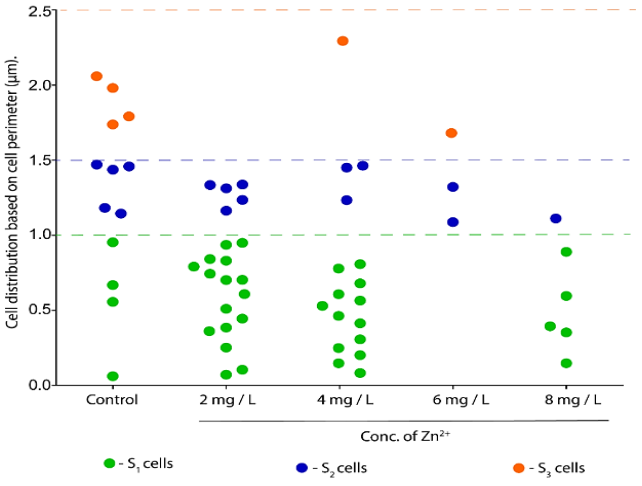

Figure 4 Zn^{2+} alters the *S. Platensis* cell population: In HM treatment, >4 mg/L of Zn^{2+} breaks the S_3 cell population into smaller fragments and distributer smaller perimerter categories like S_2 and S_1. When the Zn^{2+} increases with fragmenting the cells into smaller fragments.

The results from ImageJ analysis for cells treated with Zn^{2+} indicate that the number of cells for categories S_1, S_2, and S_3 (Figure 4). In the control (untreated) sample, there equal distribution of cells of all perimeter (S_1= 4 cells, S_2= 5 cells, and S_3= 4 cells). At lower concentration 4 mg/L of Zn^{2+}, (S_1= 13 cells, S_2= 3 cells, and S_3= 1 cells) where the distribution of the S3 cells was found at a higher perimeter. However, at a higher concentration of 8 mg/L of Zn^{2+}, only cells at category (S_1= 8 cells and S_2= 1cell) were found. Taken together, it is clear that a lower concentration of Zn^{2+} (≤ 4 mg/L) promotes cell growth as evident by an increase in cell perimeter, however, a higher concentration of Zn^{2+} (> 4 mg/L) disintegrates the S_3 cells and was distributed to S_1 and S_2 category. There is an increase in the number of trichomes in the S_1 categories owing to a reduction in growth and fragmentation of *S.platensis* caused by Zn^{2+} (Djearamane et al., 2018). In a prior study, treatment of Spirulina with ZnO nanoparticles caused fragmentation of the trichomes . Another study with the treatment of ZnSO4 showed a reduction in the number of spirals in *S. platensis* (Choudhary et al., 2007).

3.3 Cell perimeter decreases in the increase in HM concentration

ImageJ was used to compute the average perimeter of cells in the trichome stage changes due to the effect of HM. The Cu^{2+} concentration (≤ 2 mg/L) increases the average cell perimeter from ~1.33 µm to ~2.64 µm. However, higher Cu^{2+} ions concentration, 5 mg/L cleaves the larger cells to smaller fragments, and their average cell perimeter was reduced to ~0.38 µm. Similarly, Zn^{2+} concentrations (≤ 6 mg/L) increases the average cell perimeter from ~1.33 µm to ~1.81 µm, respectively, and higher Zn^{2+} ions concentration,10 mg/L cleaves the larger cells to smaller fragments, and their average cell perimeter was reduced to ~0.11 µm. From the aforementioned, imaging studies resembles the effect of HM on *S. Platensis* growth and are also toxic on higher HM concentrations which cleave the longer trichome into debris (Cepoi et al., 2020) (Figure 5).

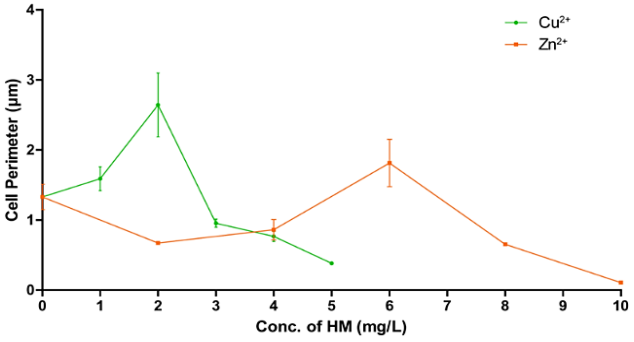

Figure 5 Effect of Cu^{2+} and Zn^{2+}on cell perimeter: In HM treatment, Cu^{2+} and Zn^{2+} enhances the cell growth of *S. Platensis* till a certain concentration, 2 mg/L, and 6 mg/L and beyond that concentration it becomes cytotoxic to the cells and cleaves the cells into smaller debris.

3.4 Image analysis as an alternative tool for cell sorting

This work demonstrates that an image analysis technique can be used not only to count the cells but also to measure and quantify the cellular geometric parameters. In this study cells were categorized by the number of spirals of the trichome and analyzed using ImageJ. Thus, this study demonstrates how one can effectively calculate the geometric parameters of cells (such as *S. platensis*) of irregular geometry. Thus, proving that those irregular shapes can also be quantified and compared. Therefore, these methods stand as an example for a cost-effective way of analysis and can potentially eliminate the need for sophisticated instruments such as flow cytometry that are not only expensive but also require frequent calibrations when using cell types of irregular geometry (Hunka et al., 2020). Thus, the findings from this study show that ImageJ can be used to effectively monitor the cells for

use in various applications. One such use is to increase biomass for the production of food supplements and the other is to aid in bioremediation and to serve as animal feed (Chen et al., 2011). In moving forward, this high-throughput image analysis technique can be further integrated into the miniaturized image capturing devices such as foldscope, such an approach would further result in a tremendous reduction in cost (Cybulski et al., 2014).

Studies have demonstrated the possibility of using MATLAB-based techniques to quantify the changes in *E. faecalis* protein localization pattern upon treatment with antimicrobial peptides (Kandaswamy et al., 2013). Although earlier studies have reported that compounds such as phytochemicals from tropical plants and nanoparticles (Govindarajan, Selvaraj, et al., 2022; Saravanan et al., 2020; Sivaramakrishnan et al., 2019) can target or kill bacterial cells but those studies were limited to few (1-10) compounds due to lack of fully automated high-throughput image analysis methods. Apart from screening, one can also take advantage of image analysis tools to perform phenotypic analysis that would result in the identification of bacterial pathotypes (Govindarajan & Kandaswamy, 2022; Govindarajan et al., 2020; Shanmugasundarasamy et al., 2022), which will be immensely helpful in the identification of water-borne pathogens for environmental water quality monitoring.

4.0 Conclusion

In summary, this study shows that HMs such as Cu^{2+} and Zn^{2+} can promote the growth of *S. Platensis* only at low concentration ($Cu^{2+} <$ 3 mg/L and $Zn^{2+} <$ 8 mg/L) but becomes toxic and leads to fragmented cellular structure at high concentrations ($Cu^{2+} \geq$ 3 mg/L and $Zn^{2+} \geq$ 8 mg/L). In addition, our image analysis technique clearly distinguishes between fragmented cell populations from unfragmented cells. Therefore, this approach can be also used to screen for compounds that can target various pathogenic bacterial strains.

Acknowledgment

The authors gratefully acknowledge the foldscope research grant from the Department of Biotechnology (DBT) SAN No: 102/IFD/SAN/4849/201718 Dated:16. Mar.2018. KK is supported by the DST SERB Start-Up Research Grant (File Number: SRG/2019/000094) from the Government of India.

Conflict of interest

The authors declare that they have no conflict of interest.

Ethical approval

This article does not contain any human study.

Data Availability Statement

The datasets generated during and/or analysed during the current study are available from the corresponding author on reasonable request

Reference

Akao, P., Cohen-Yaniv, V., Peretz, R., Kinel-Tahan, Y., Yehoshua, Y., & Mamane, H. (2019). Effect of ozonation on *Spirulina platensis* filaments by dynamic imaging particle analysis. Biomass and Bioenergy, 127, 105247.

Ali, S. K., & Saleh, A. M. (2012). Spirulina-an overview. International journal of Pharmacy and Pharmaceutical sciences, 4(3), 9-15.

Ayangbenro, A. S., & Babalola, O. O. (2017). A new strategy for heavy metal polluted environments: a review of microbial biosorbents. International journal of environmental research and public health, 14(1), 94.

Bezuidenhout, C. (2018). Near infrared hyperspectral imaging: a rapid method for the differentiation of maize ear rot pathogens on growth media. Stellenbosch: Stellenbosch University,

Bhuyar, P., Hong, D. D., Mandia, E., Rahim, M. H. A., Maniam, G. P., & Govindan, N. (2019). Desalination of polymer and chemical industrial wastewater by using green photosynthetic microalgae, *Chlorella* sp. Maejo International Journal of Energy and Environmental Communication, 1(3), 9-19.

Bhuyar, P., Trejo, M., Dussadee, N., Unpaprom, Y., Ramaraj, R., & Whangchai, K. (2021). Microalgae cultivation in wastewater effluent from tilapia culture pond for enhanced bioethanol production. Water Science and Technology, 84(10-11), 2686-2694.

Cepoi, L., Zinicovscaia, I., Rudi, L., Chiriac, T., Miscu, V., Djur, S., . . . Nekhoroshkov, P. (2020). Growth and heavy metals accumulation by *Spirulina platensis* biomass from multicomponent copper containing synthetic effluents during repeated cultivation cycles. Ecological Engineering, 142, 105637.

Collins, T. J. (2007). ImageJ for microscopy. Biotechniques, 43(S1), S25-S30.

Coltelli, P., Barsanti, L., Evangelista, V., Frassanito, A. M., & Gualtieri, P. (2014). Water monitoring: automated and real time identification and classification of algae using digital microscopy. Environmental Science: Processes & Impacts, 16(11), 2656-2665.

Cybulski, J. S., Clements, J., & Prakash, M. (2014). Foldscope: Origami-Based Paper Microscope. PLOS ONE, 9(6), e98781. doi:10.1371/journal.pone.0098781

Deniz, F., Saygideger, S. D., & Karaman, S. (2011). Response to copper and sodium chloride excess in *Spirulina* sp. (cyanobacteria). Bull Environ Contam Toxicol, 87(1), 11-15. doi:10.1007/s00128-011-0300-5

Djearamane, S., Lim, Y. M., Wong, L. S., & Lee, P. F. (2018). Cytotoxic effects of zinc oxide nanoparticles on cyanobacterium *Spirulina (Arthrospira) platensis*. PeerJ, 6, e4682. doi:10.7717/peerj.4682

Georg, M., Fernández-Cabada, T., Bourguignon, N., Karp, P., Peñaherrera, A. B., Helguera, G., . . . Mertelsmann, R. (2018). Development of image analysis software for quantification of viable cells in microchips. PLOS ONE, 13(3), e0193605. doi:10.1371/journal.pone.0193605

Ghensi, P., Bressan, E., Gardin, C., Ferroni, L., Soldini, M. C., Mandelli, F., . . . Zavan, B. (2017). The biological properties of OGI surfaces positively act on osteogenic and angiogenic commitment of mesenchymal stem cells. Materials, 10(11), 1321.

Govindarajan, D. K., & Kandaswamy, K. (2022). Virulence factors of uropathogens and their role in host pathogen interactions. The Cell Surface, 8, 100075.

Govindarajan, D. K., Meghanathan, Y., Sivaramakrishnan, M., Kothandan, R., Muthusamy, A., Seviour, T. W., & Kandaswamy, K. (2022). *Enterococcus faecalis* thrives in dual-species biofilm models under iron-rich conditions. Archives of Microbiology, 204(12), 1-11.

Govindarajan, D. K., Selvaraj, V., Selvaraj, A. S. J. M., Hameed, S. S., Pandiarajan, J., & Veluswamy, A. (2022). Green synthesis of silver micro-and nano-particles using phytochemical extracts of Cymbopogon citratus exhibits antibacterial properties. Materials Today: Proceedings.

Govindarajan, D. K., Viswalingam, N., Meganathan, Y., & Kandaswamy, K. (2020). Adherence patterns of Escherichia coli in the intestine and its role in pathogenesis. Medicine in Microecology, 100025.

Guberman, J. M., Fay, A., Dworkin, J., Wingreen, N. S., & Gitai, Z. (2008). PSICIC: Noise and Asymmetry in Bacterial Division Revealed by Computational Image Analysis at Sub-Pixel Resolution. PLoS Computational Biology, 4(11), e1000233. doi:10.1371/journal.pcbi.1000233

Hunka, J., Riley, J. T., & Debes, G. F. (2020). Approaches to overcome flow cytometry limitations in the analysis of cells from veterinary relevant species. BMC veterinary research, 16(1), 1-11.

Chen, X., Zheng, B., & Liu, H. (2011). Optical and digital microscopic imaging techniques and applications in pathology. Anal Cell Pathol (Amst), 34(1-2), 5-18. doi:10.3233/acp-2011-0006

Chilambi, G. S., Hinks, J., Matysik, A., Zhu, X., Choo, P. Y., Liu, X., . . . Rice, S. A. (2020). *Enterococcus faecalis* Adapts to Antimicrobial Conjugated Oligoelectrolytes by Lipid Rearrangement and Differential Expression of Membrane Stress Response Genes. Frontiers in microbiology, 11, 155.

Choudhary, M., Jetley, U. K., Abash Khan, M., Zutshi, S., & Fatma, T. (2007). Effect of heavy metal stress on proline, malondialdehyde, and superoxide dismutase activity in the cyanobacterium *Spirulina platensis*-S5. Ecotoxicol Environ Saf, 66(2), 204-209. doi:10.1016/j.ecoenv.2006.02.002

Kandaswamy, K., Liew, T. H., Wang, C. Y., Huston-Warren, E., Meyer-Hoffert, U., Hultenby, K., . . . Kline, K. A. (2013). Focal targeting by human β-defensin 2 disrupts localized virulence factor assembly sites in *Enterococcus faecalis*. Proc Natl Acad Sci U S A, 110(50), 20230-20235. doi:10.1073/pnas.1319066110

Karthiyayini, R., & Shenbagavadivu, N. (2020). Retinal Image Analysis for Ocular Disease Prediction Using Rule Mining Algorithms. Interdisciplinary Sciences: Computational Life Sciences. doi:10.1007/s12539-020-00373-9

Meng, H., Xia, Y., & Chen, H. (2012). Bioremediation of surface water co-contaminated with zinc (II) and linear alkylbenzene sulfonates by Spirulina platensis. Physics and Chemistry of the Earth, Parts A/B/C, 47, 152-155.

Palanisamy, K. M., Paramasivam, P., Jayakumar, S., Maniam, G. P., Rahim, M. H. A., & Govindan, N. (2021). Economical cultivation system of microalgae *Spirulina platensis* for lipid production. In IOP Conference Series: Earth and Environmental Science (Vol. 641, No. 1, p. 012022). IOP Publishing.

Rishi, N. R., & Rana, N. (2015). Particle size and shape analysis using Imagej with customized tools for segmentation of particles. Int J Comput Sci Commun Netw, 4, 23-28.

Saravanan, Y., Devaraj, B. S., Velusamy, N. K., Soundirarajan, P. S., & Kandaswamy, K. (2020). Phytochemical Extracts of Leucas aspera and *Dahlia pinnata* Exhibit Antimicrobial Properties in Escherichia coli and Enterococcus faecalis. Current Biotechnology, 9(4), 297-303.

Shanmugasundarasamy, T., Govindarajan, D. K., & Kandaswamy, K. (2022). A review on pilus assembly mechanisms in Gram-positive and Gram-negative bacteria. The Cell Surface, 8, 100077.

Schindelin, J., Arganda-Carreras, I., Frise, E., Kaynig, V., Longair, M., Pietzsch, T., . . . Cardona, A. (2012). Fiji: an open-source platform for biological-image analysis. Nat Methods, 9(7), 676-682. doi:10.1038/nmeth.2019

Sivaramakrishnan, M., Kothandan, R., Govindarajan, D. K., Meganathan, Y., & Kandaswamy, K. (2020). Active microfluidic systems for cell sorting and separation. Current Opinion in Biomedical Engineering, 13, 60-68.

Sivaramakrishnan, M., Sharavanan, V. J., Govindarajan, D. K., Meganathan, Y., Devaraj, B. S., Natesan, S., . . . Kandaswamy, K. (2019). Green synthesized silver nanoparticles using aqueous leaf extracts of *Leucas aspera* exhibits antimicrobial and catalytic dye degradation properties. SN Applied Sciences, 1(3), 208.

Tchounwou, P., Yedjou, C., Patlolla, A., & Sutton, D. (2012). Heavy metal toxicity and the environment in Molecular, clinical and environmental toxicology, vol 101 (ed. Luch, A.) 133–164. In: Springer.

Wang, Z. P., & Zhao, Y. (2005). Morphological reversion of *Spirulina (Arthrospira) platensis* (Cyanophyta): from linear to helical 1. Journal of Phycology, 41(3), 622-628.

Zinicovscaia, I., Safonov, A., Ostalkevich, S., Gundorina, S., Nekhoroshkov, P., & Grozdov, D. (2019). Metal ions removal from different type of industrial effluents using *Spirulina platensis* biomass. International journal of phytoremediation, 21(14), 1442-1448.